

# RADIONUCLIDE SORPTION AT YUCCA MOUNTAIN, NEVADA - A DEMONSTRATION OF AN ALTERNATE APPROACH FOR PERFORMANCE ASSESSMENT

David R. Turner, Roberto T. Pabalan, James D. Prikryl, and F. Paul Bertetti

Center for Nuclear Waste Regulatory Analyses, 6220 Culebra Road, San Antonio, Texas 78238

## ABSTRACT

An approach is developed for including aspects of mechanistic models of radionuclide sorption into performance assessment (PA) calculations. Water chemistry data from the vicinity of Yucca Mountain (YM), Nevada are screened and used to calculate the ranges in key parameters that could exert control on radionuclide sorption behavior. Using a diffuse-layer surface complexation model, sorption parameters for Np(V) and U(VI) are calculated based on the chemistry of each water sample. Model results suggest that lognormal probability distribution functions (PDFs) of sorption parameters are appropriate for most of the samples; the total calculated range is almost five orders of magnitude for Np(V) sorption and nine orders of magnitude for U(VI) sorption, but most samples fall in a narrower range. Finally, statistical correlation between the calculated Np(V) and U(VI) sorption parameters can be included as input into PA sampling routines, so that the value selected for one radionuclide sorption parameter is conditioned by its statistical relationship to the others. The approaches outlined here can be adapted readily to current PA efforts, using site-specific information to provide geochemical constraints on PDFs for radionuclide transport parameters.

## INTRODUCTION

Current performance assessments (PA) for the proposed high-level radioactive waste (HLW) repository at Yucca Mountain, Nevada (YM) rely on empirical parameters such as distribution coefficients ( $K_D$ ) to describe radionuclide sorption. Each radioelement is assigned a  $K_D$  probability distribution function (PDF) that is typically based on either batch experiments for a limited number of water chemistries or expert judgement. During PA calculations, each PDF is sampled for multiple realizations to estimate dose to a critical group [1,2]. It is assumed that sampled  $K_D$  values are constant for each hydrostratigraphic unit and do not vary with time in each realization. It is further assumed in the sampling procedures used in some PA models [2], that the sorption parameters for the radionuclides of concern are statistically independent of one another. Experimental and modeling studies indicate, however, that sorption behavior (and the parameter values that describe it) is strongly dependent on physical and chemical properties along transport paths [3-5]. It is therefore difficult to extrapolate  $K_D$  values beyond experimental conditions with any quantifiable certainty in PA calculations [6]. This also means that there is an underlying link that is dependent on variations in the chemistry of the system at YM that may be used to correlate the sorption behavior of different radioelements. The purpose of this study is to outline an approach that incorporates aspects of detailed geochemical models in estimating  $K_D$  for radionuclide transport at YM, and to describe how it may be implemented to represent the chemical effects on sorption behavior more accurately in the PA abstraction process.

## SORPTION MODELING APPROACHES

### Key Geochemical Parameters

The distribution (or sorption) coefficient ( $K_D$ ) is a convenient empirical ratio for representation of sorption data and is commonly used to represent retardation in transport models in PA. The  $K_D$  (mL/g) is defined as:

$$K_D \text{ (mL/g)} = \frac{\text{equilibrium mass of radionuclide sorbed on solid}}{\text{equilibrium mass of radionuclide in solution}} \times \left(\frac{V}{M}\right) \quad [1]$$

where  $V$  is the volume of solution in mL, and  $M$  is the mass of solid in g. The use of  $K_D$  has the effect of normalizing sorption results to the solid-mass to solution-volume ( $M/V$ ) ratio used in batch experiments.

Experimental and modeling results show that actinide sorption is important under conditions that favor aqueous actinyl-hydroxy complexes [7,8]. Geochemical conditions that inhibit actinide hydrolysis, such as low pH and

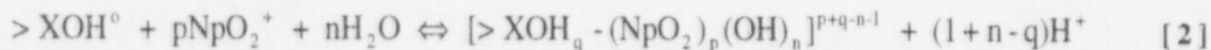
the presence of carbonate, tend to suppress sorption. The similarity in the pH-dependence of actinide sorption on a wide variety of minerals of distinct surface properties suggests that actinide sorption is not sensitive to the surface charge characteristics of the sorbent as compared to the effect of changing the total number of available sites [7,8].

Mineral specific surface area ( $A$ ) measured by gas adsorption (e.g.,  $N_2$ -BET) methods can be used as a relative measure of the number of sorption sites. Experimental data suggest that the magnitudes of actinide sorption (at a specific pH, initial radionuclide concentration, and  $PCO_2$ ) are the same for different minerals if normalized to an "effective" surface area ( $A'$ , in  $m^2/g$ ) available for sorption. Normalized to surface area, sorption can be expressed in terms of the parameter  $K_A$  ( $mL/m^3$ ) such that  $K_A = K_D/A'$  [7,8]. For nonporous minerals such as quartz and  $\alpha$ -alumina,  $A'$  can be assumed equal to the  $N_2$ -BET measured surface area. In clays, where internal sites are not likely accessible for actinide sorption, assuming  $A'$  of the variably charged edge sites is equal to about 10 percent of the total area measured by  $N_2$ -BET, similar to estimates based on titration of montmorillonite [9], matches the sorption curves for nonporous minerals [7,8].

### Surface Complexation Modeling Approaches

The effects of chemistry on actinide sorption behavior suggest that sorption parameters in PA can be constrained by geochemical models capable of accounting for the influence of varying physicochemical conditions. A class of models that has been used with success in modeling pH-dependent sorption is the electrostatic surface complexation model (SCM) [5,6]. SCMs are based on the assumption of analogous behavior between aqueous complex formation in the bulk solution and formation of surface complexes with amphoteric binding sites at the mineral-water interface. Surface reactions are written for sorbing species, and mass action and mass balance relations for the surface reactions and bulk aqueous system are used to determine sorption at the mineral surface. Of the different SCMs, the Diffuse-Layer Model (DLM) is perhaps the simplest, using a two-layer representation of the mineral-water interface. The details of the DLM and the simplified approach used in this study to model actinide sorption are described elsewhere [5,6,10,11]; only a brief overview is presented here.

In using the DLM, a generalized pH-dependent sorption reaction between aqueous actinides, such as  $Np(V)$ , and a variably charged surface sorption site is written in the form:



where  $q$  is the protonation state of the sorption site ( $q=0, 1, \text{ or } 2$  for deprotonated, neutral, and protonated sites, respectively), and  $p$  and  $n$  are the reaction coefficients for  $NpO_2^+$  and  $H_2O$ , respectively.  $NpO_2^+$  represents the aqueous neptunyl species, and  $[>XOH_q - (NpO_2)_p(OH)_n]^{p+q-n-1}$  represents the  $Np(V)$  surface complex. Similar reactions can be written for other actinides. In the electrostatic DLM approach, coulombic terms are incorporated into the mass action expressions for surface reactions of the type given in Equation [2].

The dependence of actinide sorption on pH and  $PCO_2$  is a consequence of mass action and equilibrium chemistry in the actinide- $H_2O$ - $CO_2$ -mineral system. In a qualitative sense, an increase in the activity of  $NpO_2^+$  (or similarly other actinides) drives the equilibrium reaction in Equation [2] forward (increasing sorption). The presence of a complexing ligand, such as dissolved carbonate, tends to cause the formation of aqueous actinide complexes in competition with the sorbing surface. Competition by a carbonate ligand for the available actinide increases with increasing pH, reducing the aqueous activity of  $NpO_2^+$  and driving the reaction in the opposite direction (decreasing sorption). Because the DLM provides information on the distribution of a given radioelement between the sorbed and aqueous phases, model results can be used to calculate  $K_D$  values as a function of variations in chemistry.

### REGIONAL GROUNDWATER CHEMISTRY

To construct a mass action/mass balance simulation of radioelement distribution at YM using the DLM, some estimate of site-specific water chemistry is necessary. One source of these data is the compilation of [12] that includes major and minor element analyses for over 3700 samples compiled over several decades for the region surrounding YM. For this study, it has been assumed that the ranges of values of the chemical parameters reported in [12] represent the variation that can be expected along potential flow paths in the YM hydrologic system during the postclosure period. Potential changes to the chemistry of the YM region due to the emplacement of HLW are neglected. Based

on geochemical criteria presented in [13], a series of steps listed in Table I was used to develop a refined dataset suitable for geochemical sorption modeling. An additional screening criterion included limiting the study to post-1960 analyses, which were assumed to be more traceable and reliable. The study was also limited to those waters within an area with UTM coordinates listed in Table I. This area is much larger than the flow model used in typical YM PA [1,2], but includes the most likely flow paths to the location of potential receptor groups downgradient from YM [2], current natural discharge points at Ash Meadows and Franklin Lake Playa, and paleodischarge points near Crater Flat. The resulting dataset contains 460 water analyses collected from 238 separate locations.

Regional Groundwater - Measured Geochemical Parameters

**Table I.** Screening and culling criteria as modified from [13].

Elimination Criteria	Analyses eliminated	Remaining analyses (from 3733)
No reported pH; pH <5 or pH >10	1708	2025
No reported Ca	121	1904
No reported Mg	127	1777
No reported Cl	9	1768
No reported SO <sub>4</sub>	21	1747
No reported Na	44	1703
No reported HCO <sub>3</sub> or CO <sub>3</sub>	405	1298
Not charge balanced ( $\pm 10\%$ )	23	1275
No collection date reported	82	1193
Collected before 1960	165	1028
Mg > Ca	72	956
UTM coordinates: 4,000,000N to 4,100,000N 500,000E to 600,000E	496	460

The database of water chemistries developed in this study can be used to identify ranges and distribution types for parameters such as pH and total inorganic carbon (C<sub>T</sub>) that are likely to exert control on radioelement sorption behavior [3-8,14] in the ambient hydrochemical system at YM. It is important to remember that water samples are typically integrated over a large interval in the well, and local horizons of higher or lower component concentration may not be distinguishable.

For the culled database (n = 460 samples), the minimum and maximum groundwater pH are 6.3 to 9.6 (Table II). The mean and median are nearly identical, and the data yield a straight line when plotted on normal paper, suggesting a normal distribution. It is noted in [12] that there was no attempt to distinguish between laboratory and field pH measurements; uncertainties due to degassing of CO<sub>2</sub> prior to analysis may exist and not be discernible in the dataset. Groundwater C<sub>T</sub> in the YM system covers a broad range from 6.8 to greater than 10,000 mg/L, and calculated equilibrium ionic strength ranges from  $4.3 \times 10^{-4}$  to about 1.3 molal. The number of analyses with high C<sub>T</sub> (> 1,000 mg/L) and/or high ionic strength (> 0.5 molal) is small (fewer than 10 out of 460 samples), but gives a positive skewness to the distributions (Table II). These samples are brines from playa deposits south of YM, and therefore are likely not to represent deep regional groundwaters. Without treatment, the brines are also unusable as a potable drinking water source.

**Table II.** Descriptive statistics of groundwater chemical parameters [12].

	pH (std units)	C <sub>T</sub> (mg/L)	Ion. Str. (molal)
Mean	7.83	295.76	$1.93 \times 10^{-2}$
Median	7.8	245.0	$8.56 \times 10^{-3}$
Std.Dev.	0.45	525.99	$9.86 \times 10^{-2}$
Kurtosis	1.75	270.67	139.44
Skewness	0.43	15.03	11.65
Minimum	6.3	6.80	$4.34 \times 10^{-4}$
Maximum	9.6	10140.0	$1.31 \times 10^{-0}$
Count	460	460	460

**RADIONUCLIDE SORPTION MODELING FOR THE YUCCA MOUNTAIN SYSTEM**

The type and limits to PDFs used to describe sorption parameter uncertainty in PA are usually based on informal expert elicitations [1] and batch experiments with crushed rock and a limited suite of groundwater chemistries [2]. Computational requirements limit the explicit incorporation of geochemical sorption models into current PA codes,

and it is likely that the use of PDFs will continue in the next generation of PA codes. It may be possible, however, to apply detailed geochemical sorption models "off-line" to provide PDF constraints in PA transport models that reflect the site-specific effects of key geochemical parameters on radionuclide sorption. To demonstrate this approach, sorption of Np(V) and U(VI) was modeled using the DLM and hydrochemical information specific to YM.

#### Model Setup

Modeling of Np(V) and U(VI) sorption was

performed using the DLM option in the geochemical code MINTEQA2 [15]. Data from each chemical analyses in the culled database were written to a MINTEQA2 input file. The pH and temperature were fixed at the measured values, Eh was unspecified due to a lack of measured data, and measured Fe was assumed to be entirely Fe<sup>3+</sup>. Surface sorption reactions for the actinide-H<sub>2</sub>O-CO<sub>2</sub>-montmorillonite system (Table III), based on experimental work [16,17], were added to the MINTEQA2 input file. Montmorillonite was selected since it is a common alteration mineral in the volcanic tuffs at YM [18] and is potentially a strong sorber of actinides. In the absence of data on solid-mass to solution-volume ratios in the YM system, it was assumed that M/V = 1 g/L. For simplicity, ion exchange reactions, which may be less significant for neptunium and uranium at the observed groundwater pH [16,17], were not included in the model and only surface complexation was considered. It is important to note that, although full aqueous speciation is incorporated in the model, the only surface reactions considered are protonation/deprotonation and actinide sorption reactions. Calculated changes in sorption behavior are therefore limited to those resulting from changes in aqueous speciation of the radionuclide due to complexing with ligands in the groundwater [16,17]; direct competition for available surface sites is neglected.

Total dissolved and sorbed concentrations for Np(V) and U(VI) were extracted from the MINTEQA2 output file for each of the 460 groundwater analyses.  $K_A$  was calculated assuming  $A' = 9.7 \text{ m}^2/\text{g}$  for montmorillonite (10 percent of the N<sub>2</sub>-BET surface area) [16,17]. Additional information in the MINTEQA2 output file that may be useful in future PA calculations includes aqueous species concentrations, equilibrium ionic strength, gas partial pressures (e.g., PCO<sub>2</sub>), and saturation indices for minerals that are in the MINTEQA2 database.

## RESULTS

### Np(V)-Montmorillonite

Calculated Np(V) sorption on montmorillonite (Table IV), expressed in terms of  $K_A$ , is shown in Figure 1a. The calculated values of  $K_A$  (and  $K_D$ ) range over five orders of magnitude, although most of the samples fall within a range of 2-3 orders of magnitude. The maximum  $K_A$  is almost 76 mL/m<sup>2</sup> (corresponding to a maximum  $K_D$  of about 730 mL/g). The distribution is roughly lognormal for most of the samples, with a mean of about  $10^{0.74} = 5.5 \text{ mL/m}^2$  (mean  $K_D$  of  $10^{1.73} = 53 \text{ mL/g}$ ). About 95 percent of the values lie within 2 standard deviations ( $\sigma$ ) of the mean, but there is a negative skewness (Table IV) due to a small number of low values calculated for the carbonate-rich waters

**Table III.** DLM parameters used in modeling Np(V) and U(VI) sorption on montmorillonite.

Model Parameter/Surface Reaction	Mineral/Surface Parameters	
Total site concentration <sub>a</sub>	>AlOH <sup>o</sup> = 1.7 × 10 <sup>5</sup> mol sites/L >SiOH <sup>o</sup> = 2.0 × 10 <sup>5</sup> mol sites/L	
Total radionuclide concentration	1 × 10 <sup>-6</sup> molal	
Edge-Site Reactions:	Log K	
	Np(V)	U(VI)
>AlOH <sup>o</sup> + H <sup>+</sup> ⇌ >AlOH <sub>2</sub> <sup>+</sup>	8.33 <sub>b</sub>	8.33 <sub>b</sub>
>AlOH <sup>o</sup> ⇌ >AlO <sup>-</sup> + H <sup>+</sup>	-9.73 <sub>b</sub>	-9.73 <sub>b</sub>
>SiOH <sup>o</sup> ⇌ >SiO <sup>-</sup> + H <sup>+</sup>	-7.20 <sub>b</sub>	-7.20 <sub>b</sub>
>AlOH <sup>o</sup> + NpO <sub>2</sub> <sup>+</sup> + H <sub>2</sub> O ⇌ >AlO-NpO <sub>2</sub> (OH) + 2H <sup>+</sup>	-13.79 <sub>c</sub>	--
>SiOH <sup>o</sup> + NpO <sub>2</sub> <sup>+</sup> ⇌ >SiOH-NpO <sub>2</sub> <sup>+</sup>	4.05 <sub>c</sub>	--
>AlOH <sup>o</sup> + UO <sub>2</sub> <sup>2+</sup> ⇌ >AlO-UO <sub>2</sub> <sup>+</sup> + H <sup>+</sup>	--	2.70 <sub>d</sub>
>SiOH <sup>o</sup> + UO <sub>2</sub> <sup>2+</sup> ⇌ >SiO-UO <sub>2</sub> <sup>+</sup> + H <sup>+</sup>	--	2.60 <sub>d</sub>
>AlOH <sup>o</sup> + 3UO <sub>2</sub> <sup>2+</sup> + 5H <sub>2</sub> O ⇌ >AlO-(UO <sub>2</sub> ) <sub>3</sub> (OH) <sub>5</sub> <sup>o</sup> + 6H <sup>+</sup>	--	-14.95 <sub>d</sub>
>SiOH <sup>o</sup> + 3UO <sub>2</sub> <sup>2+</sup> + 5H <sub>2</sub> O ⇌ >SiO-(UO <sub>2</sub> ) <sub>3</sub> (OH) <sub>5</sub> <sup>o</sup> + 6H <sup>+</sup>	--	-15.29 <sub>d</sub>

- Al/Si ratio of 0.83 [8].
- Ref. [11]
- Ref. [17]
- Ref. [16]

discussed previously. The similarity of the mean and median values suggests the mean is not overly affected by the extremes of the distribution. Plotting  $K_D$  against measured pH and  $C_T$  shows the effect of system chemistry on sorption. The calculated pH-dependence is very similar to controlled laboratory experiments [17] that show a sharp increase in maximum sorption over a narrow pH range of about 7.5 to 9 (Figure 1b). Calculated sorption also decreases with increasing  $C_T$ , reflecting the effects of aqueous neptunyl-carbonate complexation.

#### U(VI)-Montmorillonite Sorption

Calculated U(VI)-montmorillonite sorption (Table IV), expressed as  $K_A$ , is shown in Figure 2a. The distribution is approximately lognormal, with a total range of nine orders of magnitude that is much broader than the  $K_A$  (and  $K_D$ ) distribution for Np(V)-montmorillonite. Like Np(V)-montmorillonite, however, most of the calculated U(VI) sorption parameters are concentrated in a narrower range that spans about 4-5 orders of magnitude. The maximum  $K_A$  is about  $10^{2.57}$  mL/m<sup>2</sup> ( $K_D = 10^{3.56}$  mL/g) (Table IV). There is a negative skewness, due to low values calculated for the carbonate-rich groundwaters. As with Np(V)-montmorillonite sorption, about 95 percent of the values lie within  $2\sigma$  of the mean ( $K_A = 10^{0.03}$  mL/m<sup>2</sup>;  $K_D = 10^{0.002}$  mL/g) and the similarity to the median suggests that the mean is not overly influenced by extreme values. In contrast to the positive correlation shown in Figure 1b, U(VI)-montmorillonite shows a decrease

**Table IV.** Descriptive statistics of calculated Np(V)- and U(VI)-montmorillonite sorption for groundwater chemistries in [12]. Derived using DLM with parameters in Table III.

	Np(V)		U(VI)	
	Log $K_A$ (mL/m <sup>2</sup> )	Log $K_D$ (mL/g)	Log $K_A$ (mL/m <sup>2</sup> )	Log $K_D$ (mL/g)
Mean	0.74	1.73	-0.03	0.96
Median	0.77	1.76	0.002	0.99
Std. Dev.	0.42	0.42	0.98	0.98
Kurtosis	26.58	26.58	12.93	12.93
Skewness	-3.56	-3.56	-2.32	-2.32
Minimum	-3.26	-2.28	-6.84	-5.85
Maximum	1.88	2.86	2.57	3.56
Count	460	460	460	460

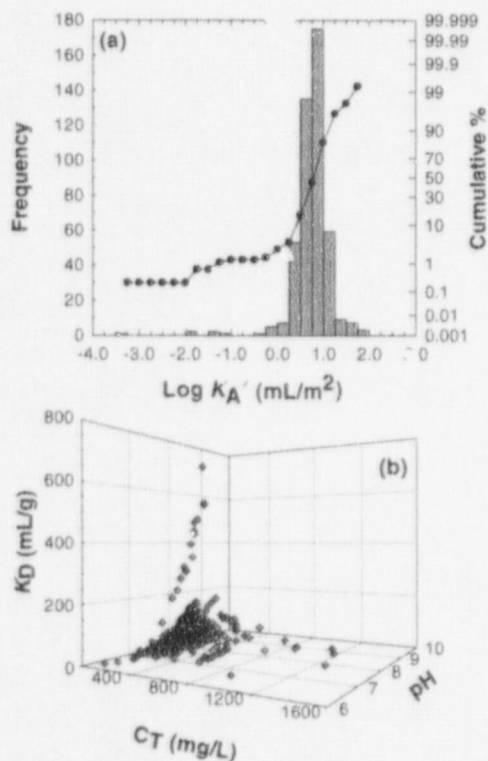


**Figure 1.** Distribution of DLM-calculated (a)  $K_A$  (in mL/m<sup>2</sup>); (b)  $K_D$  (in mL/g), for the Np(V)-montmorillonite system as a function of groundwater pH and  $C_T$ .

in sorption with increasing pH for the YM groundwaters (Figure 2b), reflecting the higher pH for Np(V) hydrolysis reactions relative to U(VI) hydrolysis [7,8]. The calculated pH-dependence is very similar to controlled laboratory experimental results [16] that show a sharp decrease in sorption over a narrow pH range in the presence of aqueous carbonate. Like Np(V), there is a negative correlation between U(VI) sorption and  $C_T$ . The reduction in U(VI) sorption with increasing  $C_T$  is even more pronounced than that determined for Np(V) sorption, reflecting the effects of stronger carbonate complexation of U(VI) relative to Np(V) [7,8].

#### Incorporation of Calculated PDFs in PA

Descriptive statistics such as those in Table IV represent the type of information from detailed models that can be used to constrain sorption parameter PDFs for current PA models. Np(V) and U(VI) sorption on various aluminosilicate minerals exhibit a similar pH-dependent behavior that is independent of mineral type [7,8]. The amount of radionuclide sorbed is instead a function of mineral surface area. This suggests that the  $K_A$  distributions developed in Figures 1 and 2 for montmorillonite are valid for other aluminosilicate and silicate minerals. The magnitude of  $K_D$  for input into PA transport calculations can therefore be determined for a given mineral by multiplying the distribution in Figures 1a and 2a by  $A'$  for that mineral. For example, for quartz,  $A'$  is small (e.g.  $\sim 0.03$  m<sup>2</sup>/g [7]). Assuming that the distribution shown in Figure 1a is valid for Np(V)-quartz sorption, the mean calculated

$K_{D,Qz} = K_{A,mont} \times A'_{Qz} = (5.5 \text{ mL/m}^2) \times (0.03 \text{ m}^2/\text{g}) = 0.2 \text{ mL/g}$ . This value compares well to the low values ( $K_{D,Qz} < 1 \text{ mL/g}$ ) reported for Np(V) batch sorption studies with quartz and J-13 well water [19].

The application of calibrated sorption models also offers a way of developing a multivariate statistical correlation among sorption parameter PDFs to reflect the underlying effects of geochemistry on sorption that are not accounted for in current PA codes. For example, calculating a distribution for Np(V)- and U(VI)-montmorillonite sorption can provide a direct means of testing the bivariate correlation between Np(V) and U(VI) sorption that results from the effects of chemical variability. The relationship is not 1:1 due to differences in the aqueous speciation of Np(V) and U(VI) (dashed line in Figure 3). The correlation coefficient for  $\text{Log } K_D$  calculated for Np(V) and U(VI) is about 0.6, indicating a positive correlation in sorption behavior for these two actinides (Figure 3) due to geochemical effects alone. The correlation is weak, however ( $r^2 = 0.37$ ), and is likely influenced by a few outlier points. Nevertheless, correlation coefficients calculated in a similar manner for multiple pairings of radioelements can be included as input into the PA sampling routine; in this way, the value selected for one radioelement sorption parameter is conditioned by its statistical (and therefore geochemical) relationship to the other radioelements.

### Spatial variation in Sorption Parameters

The large range in calculated sorption parameters (Table IV) is due to spatial variability in the ambient regional groundwater chemistry at YM. One means of showing the variability in geochemical and sorption parameters is through the use of contour plots. A geographic information system (GIS) coverage was created to show the spatial variation in potential radionuclide sorption that may have an effect on PA calculations (Figure 4). Higher regions of potential sorption are due to small clusters of high pH/low carbonate waters located to the east of YM and to the southwest of Crater Flat. Calculated  $K_D$  for Np(V)-montmorillonite sorption is in the range of 25 to 100 mL/g for most of the region downgradient from YM. There is a local high in potential sorption with a northwest-southeast trend in calculated  $K_D$  that parallels trends in pH and  $\text{PCO}_2$  as well as the axis of Amargosa Valley. Contour plots of a derived parameter such as  $K_D$  should be used carefully given the large number of groundwater properties that may potentially affect the model calculations. The map also shows that even with 238 separate sample locations, sampling density is concentrated in a few areas, and generally quite sparse over much of the region of interest.

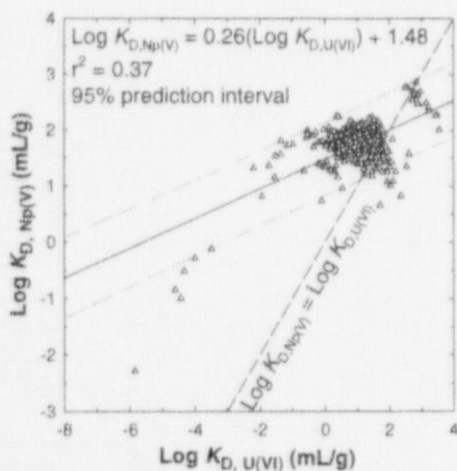


**Figure 3.** Np(V) and U(VI) distribution coefficients for montmorillonite ( $\text{Log } K_D$  in  $\text{mL/g}$ ) calculated using the DLM.

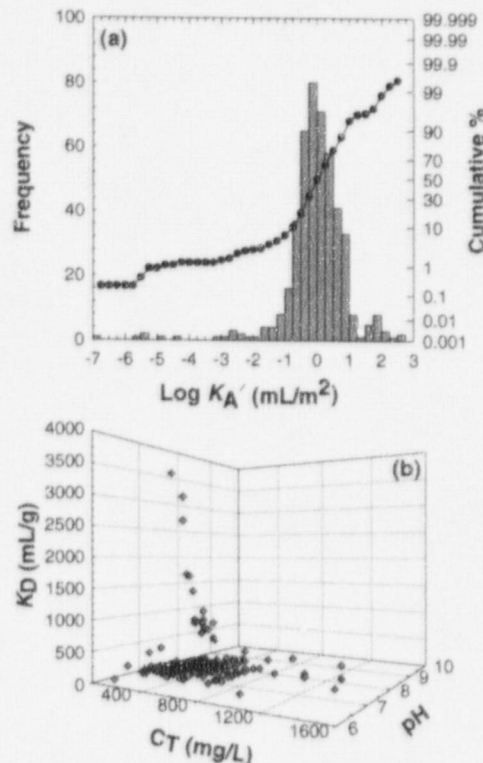


**Figure 2.** Distribution of DLM-calculated (a)  $K_A'$  (in  $\text{mL/m}^2$ ); (b)  $K_D$  (in  $\text{mL/g}$ ), for the U(VI)-montmorillonite system as a function of groundwater pH and  $C_T$ .

### SUMMARY AND CONCLUSIONS

While coupled hydrogeochemical transport codes may be used to examine particular aspects of reactive transport in detail, the additional computational burden that results from coupling equations for geochemistry and fluid flow may be excessive for the purposes of current PA calculations. The need for simplified abstractions is even more important for stochastic approaches that rely on sampling techniques and many realizations to generate complementary cumulative distribution functions that measure repository performance. Screening and culling of regional groundwater

chemistry data in the YM vicinity [12] provides a set of consistent and complete hydrochemical analyses suitable for detailed geochemical modeling of radionuclide transport processes. Using the DLM "off-line", both Np(V) and U(VI) are calculated to be weakly sorbed under most the observed groundwater conditions; the model results suggest that lognormal distributions of actinide sorption parameters are appropriate. The total ranges in calculated sorption parameters are greater than five [Np(V)] and nine [U(VI)] orders of magnitude due to changes in observed hydrochemistry alone, but much of the lower part of the range is due to a relatively small set of carbonate-rich groundwaters. The statistical relationship between the calculated Np(V) and U(VI)  $K_D$  PDFs also provides a demonstration of calculating correlation coefficients among radioelement sorption parameters. While not an explicit incorporation of geochemistry in transport calculations, this indirect means of including the effects of geochemistry does provide a step towards a more theoretical basis for sorption modeling in PA.

### Contour Map of $K_D$ for Neptunium Yucca Mountain Region

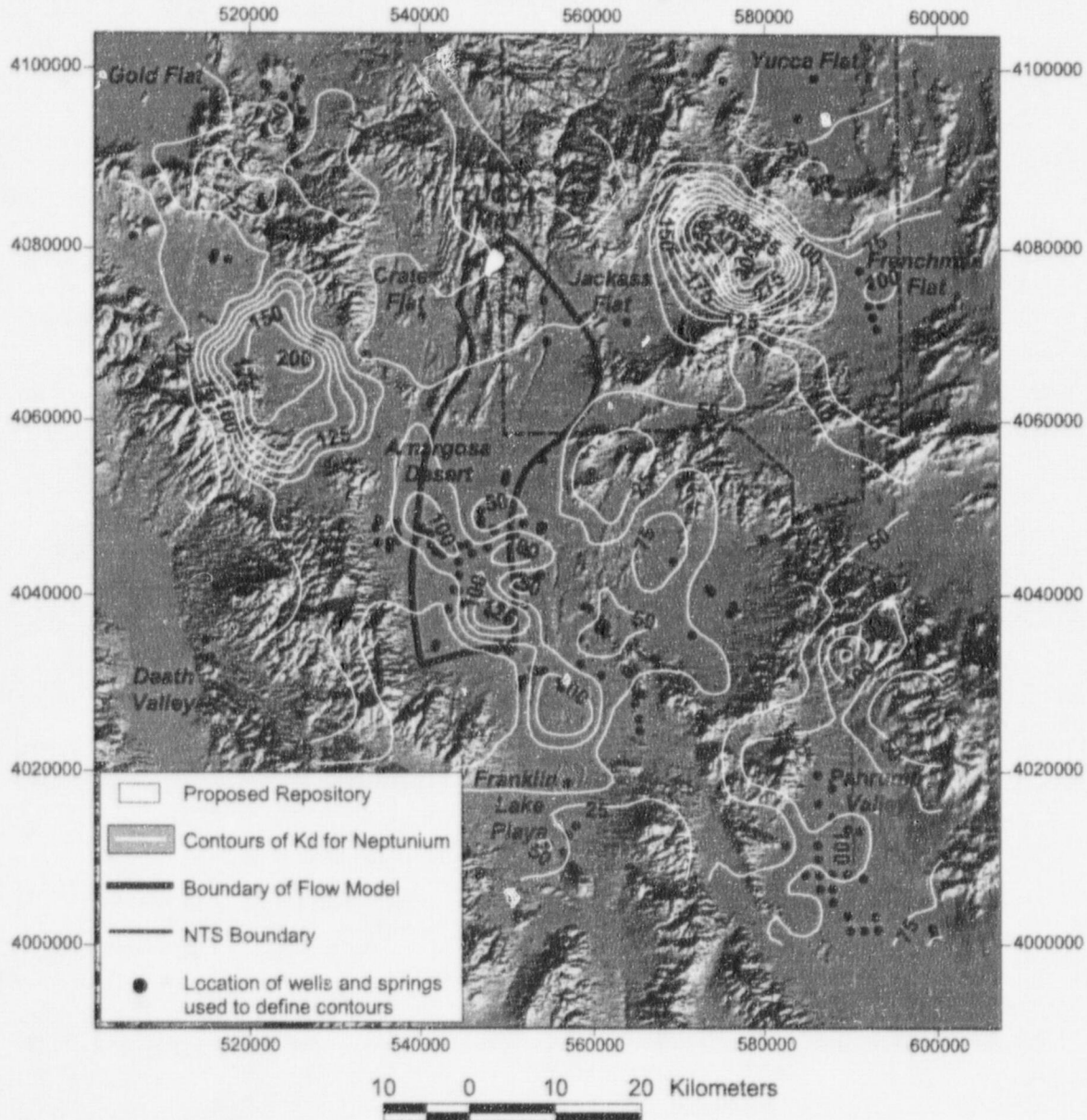


**Figure 4.** Contour map of Np(V)-montmorillonite  $K_D$  (in mL/g) calculated using the DLM with parameters from Table III and water chemistry from [12]. Contour interval = 25 mL/g. Heavy outline shows the flow model from YM (white) used in NRC PA calculations [2].

## ACKNOWLEDGMENTS

This report documents work performed by the Center for Nuclear Waste Regulatory Analyses (CNWRA) for the Nuclear Regulatory Commission (NRC) under Contract No. NRC-02-97-009. It is an independent product of the CNWRA and does not necessarily reflect the views or regulatory position of the NRC.

## REFERENCES

1. TRW Environmental Safety Systems, Inc., B00000000-01717-2200-00136, Las Vegas, NV, 1995.
2. S. Mohanty and T. McCartin, NUREG-1668, Vol. 1, Nuclear Regulatory Commission, Washington, DC, 1998.
3. D. Langmuir, Aqueous Environmental Geochemistry (Prentice Hall, Upper Saddle River, NJ, 1997).
4. D. Langmuir, in Scientific Basis for Nuclear Waste Management XX, edited by W. Gray and I. Triay (Materials Research Society Proceedings 465, Pittsburgh, PA, 1997), p. 769-780.
5. D. Turner, CNWRA 95-001, Center for Nuclear Waste Regulatory Analyses, San Antonio, TX, 1995.
6. J. Davis and D. Kent, in Reviews in Mineralogy: Vol. 23. Mineral-Water Interface Geochemistry, edited by M. Hochella, Jr. and A. White (Min. Soc. Amer., Washington, DC, 1990), p. 177-260.
7. F. Bertetti, R. Pabalan, and M. Almendarez, in Adsorption of Metals by Geomedia, edited by E. Jenne (Academic Press, Inc., New York, 1998), p. 131-148.
8. R. Pabalan, D. Turner, F. Bertetti, and J. Prikryl, in Adsorption of Metals by Geomedia, edited by E. Jenne (Academic Press, Inc., New York, 1998), p. 99-130.
9. H. Wanner, Y. Albinsson, O. Karnl, E. Wieland, P. Wersin, and L. Charlet. *Radiochimica Acta* **66/67**, 733 (1994).
10. D. Dzombak and F. Morel, Surface Complexation Modeling: Hydrous Ferric Oxide (John Wiley and Sons, New York, 1990).
11. D. Turner and S. Sassman, *Journal of Contaminant Hydrology* **21**, 311 (1996).
12. D. Perfect, C. Faunt, W. Steinkampf, and A. Turner, USGS-OFR-94-305, U.S. Geol. Survey, Denver, CO, 1995.
13. B. Hitchon and M. Brulotte, *Applied Geochemistry* **9**, 637 (1994).
14. M. Bradbury and B. Baeyens, *Journal of Colloid and Interface Science* **158**, 364 (1993).
15. J. Allison, D. Brown, and K. Novo-Gradac, EPA/600/3-91/021, Environ. Protection Agency, Athens, GA, 1991.
16. R. Pabalan and D. Turner, *Aqueous Geochemistry* **2**, 203 (1997).
17. D. Turner, R. Pabalan, and F. Bertetti, *Clays and Clay Minerals* **46**, 256 (1998).
18. D. Vaniman, D. Bish, S. Chipera, B. Carlos, and G. Guthrie, YMP Milestone 3665, Los Alamos National Laboratory, Los Alamos, NM, 1996.
19. I. Triay, C. Cotter, M. Huddleston, D. Leonard, S. Weaver, S. Chipera, D. Bish, A. Meijer, and J. Canepa, LA-12961-MS/UC-814, Los Alamos National Laboratory, Los Alamos, NM, 1996.